Bi-Doped SnO_2 Transparent Conducting Thin Films Deposited By Spray Pyrolysis: Structural, Electrical, Optical And Photo-Thermoelectric Properties

N. Khademi
Damghan University
Mohammad Bagheri-Mohagheghi (bmohagheghi@du.ac.ir)
Damghan University https://orcid.org/0000-0002-8642-7456
A. shirpay
Khatamol-anbi university

Research Article

Keywords: SnO2, Bi-doping, spray deposition, thermoelectric properties

Posted Date: September 16th, 2021

DOI: https://doi.org/10.21203/rs.3.rs-852267/v1

Version of Record: A version of this preprint was published at Optical and Quantum Electronics on February 1st, 2022. See the published version at https://doi.org/10.1007/s11082-022-03515-z.

Abstract

In this research, light and heavy Bi-doped SnO_2 thin films were prepared on glass substrates by spray pyrolysis technique. The effect of heavy doped-Bi on the structural, morphological, electrical, photo-thermo-electrical, optical properties of SnO_2 films has been investigated.

The Bi/Sn atomic ratios (**x = [Bi/Sn])** were varied from **0 to 0.30** in the spray solution.

X-ray diffraction analysis showed the formation of SnO_2 tetragonal rutile structure in low doped deposited films and amorphous structure for heavy Bi-doped SnO_2. Also, the **SnO_2-Bi_2O_3 binary** thin films were formed for **x= [Bi/Sn] =0.05**. Scanning electron microscopy (SEM) images indicated that nanostructure of the condensed films has a rectangular-particle growth toward particle- spherical growth. The Hall effect measurements have shown **n-type conductivity** in all deposited films. The lowest sheet resistance of 39.3 MΩ/□ and highest carrier concentration of **$n=4.53 \times 10^{18}$ cm^{-3}** were obtained for the thin film deposited with **x = 0.10**. The maximum of the Seebeck coefficient (**S)=325 μVK^{-1}** and figure of merit (ZT) = **1.85** was obtained for the thin film deposited with **x = 0.20**. The average transmittance of films varied over the range of **T=72%-84%.** The band gap values of samples were obtained in the range of **E_g=3.52–3.88 eV** for direct band gap. From the photoconductivity studies, the sample prepared with **x = 0.20** exhibited the highest photoconductivity among the SnO_2: Bi thin films.

Introduction

Research and innovation in the field of semiconductor physics to achieve new properties and applications for the construction of advanced and modern devices has always been a topic of interest to researchers and has allocated the largest volume of research annually. The new solid-state components, which have very high speeds in the transmission of audio and video, as well as transistors and multiple semiconductor quantum junctions, solar cells, memory components, and processing in quantum information, owe much to this research. One of these advanced and widely used materials is transparent conductive oxides (TCOs) [1–5].

Transparent conducting oxides (TCOs) have been widely studied in recent years since they have shown concurrently high optical transparency in the visible region and high electrical conductivity. According to the reported results, the best n-type TCOs are In_2O_3: Sn (ITO), SnO_2: F (FTO), ZnO: Al (AZO) films. Optical transparency of more than 90% and resistivity in the order of 10^{-4} Ω.cm have been found for these films [4–5].

Among the transparent conductive thin films, SnO_2: F (FTO) have special importance and received more attention due to its low cost of synthesis, abundance and solidity of processes, and high chemical stability. For example, they have been used in, flat-panel displays, electro-chromic devices, solar cells, electromagnetic shielding, functional glasses, and gas sensors. In heat-efficient window applications, the

TCOs are used as filters that reflect in the infrared region and remain transparent in the visible region [3, 4].

Conventional n-type TCO materials are prepared by various deposition methods such as physical vapor deposition (PVD), thermal evaporation, chemical vapor (CVD), and spray pyrolysis. However, among these deposition methods, the spray pyrolysis (SP) technique is an inexpensive method for the deposition of transparent conducting oxides and other materials such as optical selective coating, magnetic oxide materials, superconductors, and semiconductor thin films. It is a relatively simple and inexpensive technique for large-scale coatings on glass and special substrates at atmospheric pressure [5, 6]. The microstructure of the films can be affected by deposition parameters such as the substrate temperature, spray rate, and solution concentration. Lower temperatures lead to more disordered i.e. polycrystalline and amorphous states, while higher temperatures lead to increased polycrystalline grain sizes and more condensation. This technique is compatible with other conventional processes like physical vapor deposition in fabricating detectors, thin film sensors, electrochromic devices, solar cells, transparent p–n junctions, and other optoelectronic devices [5].

Recently, binary transparent oxides of n- type and p-type TCO materials have been developed such as n-Zn_2SnO_4 [7, 8], n-$MgIn_2O_4$ [9], n-$CdSb_2O_6$:Y [10], n-$ZnSnO_3$ [11], p-$CuAlO_2$ [12], p-$CuGaO_2$ [13], p-$SrCu_2O_2$ [14], p-ZnO:(Ga, N) [15] and p-NiO : Li [16, 17]. Therefore, the use of n-type and p-type TCOs in the fabrication of active elements in optoelectronic devices as transparent p–n junctions is possible [18–25].

In addition, the new impurities for the study of modified properties of tin oxide thin films such as Al [19, 26], Li [20], Co, Ni [21], Cr [22, 25], B [23], Cu [24], co-doped P and F and Sb [29–33] have been investigated; but there are few reports in our knowledge on the Bi-doping in SnO_2 transparent conducting thin films deposited by spray pyrolysis.

Bismuth is a metallic element with atomic number of 83, pentavalent with electron configuration [Xe] $4f^{14}$ $5d^{10}$ $6s^2$ $6p^3$, atomic radius r = 1.56 Å and rhombohedral structure (a = b = c; α = β = γ ≠ 90°). It has long been considered as the element with the highest atomic mass that is stable similar to lead. Additionally, bismuth has the highest Hall coefficient and when deposited in a sufficiently thin film on a substrate, bismuth is a semiconductor, rather than other metals. The most Bi-compounds in oxide and sulfide phases are Bi_2O_3, Bi_2O_5, and Bi_2S_3 [25].

SnO_2 is known as a semiconductive oxide and is used as one of the thermoelectric base materials. The mobility of the carrier in the SnO_2 is high and increases / decreases with the addition of some impurities. In order to reduce the conductivity and increase the thermal conductivity, which plays an important role in the figure of merit, heavy elements such as bismuth, antimony, etc. can be used. Since SnO_2 ceramic has a porous structure, so the thermoelectric performance of the SnO_2 system can be improved with a dense structure because the value of the electrical conductivity must be significantly improved. The addition of heavy metals has been reported to improve the thermoelectric properties of SnO_2 [33]. The thermoelectric properties of Sb-doped SnO_2 have been extensively studied [33–37], but Bi-doped SnO_2 has rarely been

studied. Bismuth and antimony are known to have similar chemical properties due to their similar positions in the periodic table of elements.

Bi^{3+} doping together increases the electrical conductivity and the Seebeck coefficient because of the combined effects of decreasing the carrier concentration and increasing the carrier mobility. In addition, heavy ion doping can effectively reduce thermal conductivity, which is important for increasing the figure of merit [38].

So, in this research, we investigate the effect of bismuth impurity on the physical properties of the SnO_2 transparent conducting thin films prepared by spray pyrolysis method. The phase structure, scanning electron microscopy (SEM) analysis, and optical, electrical, photoconductive, and thermo-electrical properties of these films were studied using X-ray diffraction (XRD), Hall measurement, Seebeck effect, Photoconductive effect, and UV–Vis absorption spectroscopy.

Experimental Procedures

2.1. Preparation of SnO_2: Bi thin films

Bi-doped SnO_2 thin films were deposited on glass substrates by spray pyrolysis technique. The details of this method have been reported elsewhere [17]. For preparation of films, the spray solutions were prepared by dissolving 0.1 mol of tin chloride: **$SnCl_4$, $5H_2O$** and bismuth nitrate: **$Bi_5O(OH)_9(NO_3)_4$** with **x= [Bi/Sn]** atomic ratio = **0, 0.05, 0.10, 0.15, 0.20, 0.30** in a solvent containing double distilled water and ethanol with a volume ratio of 1:1. For more solvability of bismuth nitrate in distilled water a few drops of nitric acid and chloric acid added to spray solution. In any step, 20 ml of the starting solutions were sprayed on glass substrates, using compressed air (3×10^5 Pa) as the carrier gas with a solution flow rate of 10 ml/min and a nozzle to substrate distance of d = 35 cm. The substrate temperature was fixed at **T = 480°C**. It should be noted that the bismuth solution is a corrosive solution, therefore, spray processes was done with a glassy nozzle. The steps for preparing SnO_2: Bi thin films are shown in Fig. 1.

2.2. Characterization

The deposited films were characterized by X-ray diffraction (XRD), Scanning electron microscopy (SEM), UV-Vis spectroscopy and electrical, optical and thermo-electric, and photoconductivity properties of films have been studied. The XRD patterns of films were recorded by D8 Advance Bruker system with Ni filtered using Cu Kα (λ = 0.15406 nm) radiation at an operating voltage of 35 KV and current of 30 mA. Surface morphology of the films was observed using a Philips XL-30 SEM system with the acceleration voltage of 20 kV.

The sheet resistance (R_S) of the films measured by two-point probe method using thermally evaporated aluminum electrodes in vacuum technique using the Edwards E-306 coating system. Then, by measuring

the sheet resistance (R_S) and the average thickness of the films (t), the electrical resistivity of the samples was calculated using the following relation:

$\rho = R_S \times t$. (1)

A Hall effect experiment was performed at room temperature T = 300 K by applying a magnetic field (B = 130 mT) perpendicular to the plane of the films to determine the concentration and the type of the majority carriers and also, resistivity (ρ) of the films. A schematic view of the Hall effect experiment is shown in Fig. 2.

To measure the thermoelectric effect, a system is used in which a temperature difference (δT) is applied to both ends of the sample using a heat source (electric heater) and a cold source (water and ice). Then, with increasing temperature, a difference in thermoelectric potential (δV, emf) appears at the two ends of the sample, which is called the thermoelectric effect. Then the seebeck coefficient is obtained from the ratio of the difference in electrical voltage to the temperature difference. The Seebeck coefficients were determined by calculating the slope of the thermoelectric (emf) versus temperature difference (δT) at the temperature range T = 300– 500 K [24].

A schematic view of the thermoelectric apparatus is shown in Fig. 3. The open circuit voltage generated by the sample was measured using a digital microvoltmeter.

The temperature difference between the two ends of the sample causes the transport of carriers from the hot to the cold end, thus creating an electric field, which gives rise to thermoelectric across the ends. The generated thermoelectric is directly proportional to the temperature gradient applied to the two ends of semiconductor thin films.

The optical measurements carried out in the range of λ = 190–1100 nm using Unico 4802 double beam spectrophotometer system. The thickness of the films (t) was controlled by deposition parameters and determined from transmission interference fringes by the Swanepoel method [17]. To study the photoconductive properties of films, samples were exposed to light radiation with a fixed intensity (4200 Lux) at a fixed distance (20 cm) using a normal light source (a tungsten fiber lamp). Then, the electrical resistance change of the prepared films was recorded.

Results And Discussion

3.1. Structural properties

The XRD patterns of films with different values of x from 0 to 0.30 are shown in Fig. 4 (a) to (e). As seen, for x = 0 and x = 0.05, films are polycrystalline corresponding to SnO_2 phase and have tetragonal rutile structure and shows preferred orientation along (211) which changes into only plane (200) at x = 0.05. Other orientations such as (110), (310) and (301) are shown, but with lower intensities. At doping level of x = 0.05, γ-Bi_2O_3 phase is also showed.

By adding Bi impurity more than x = 0.05 toward x = 0.30, the intensities of peaks decreased considerably, and film structure close to amorphous nature with a higher background. As seen in Fig. 4 (c) to (e) as the Bi-concentration is increased gradually, SnO_2 phase disappeared and unstable phases of tin oxides such as beta-SnO, Sn_3O_4 and Sn_5O_6, and also tin-bismuth oxides combined phases such as Bi_2SnO_7, and Bi_7SnO are indicated.

Regarding atomic radius of Bi^{5+} (1.56 Å) and Sn^{4+} (0.71 Å), in doping levels lower than x = 0.10, probable substitution of Bi^{5+} ions in lattice positions of Sn^{4+} is possible which results in increasing the peaks intensities. Indeed, we knew that in low doping level this is possible, even if atomic radius of impurity becomes more than atomic radius of host atom [39]. However, in doping level x = 0.10 and higher, probably, bismuth ions occupy the interstitial sites, therefore, lead to lattice disorder and defect in BTO film structure and decreasing of crystallinity of films. This suggests there is a solubility limit for Bi in SnO_2 lattice in about x = 0.10.

Estimated crystallite size (D) is calculated using the Debye–Scherrer's formula [17].

$$D = k\lambda/\beta \cos\theta \quad (2)$$

where β is the full width at half maximum of the corresponding XRD peak, k is a constant (~ 1) and θ is the Bragg angle. XRD parameters such as crystallite size (D) and the phases identified along (211) plane have summarized in Table 1.

3.2. Surface morphology

SEM micrographs of films are shown in Fig. 5. As seen, surface morphology of the films is dependent upon the Bi doping level. In the low doping level of Sn ($x \leq 0.10$), the micrographs show that the nanostructure of the condensed films has a separate single spherical crystallites and grain growth morphology, and further increasing the Bi content up to x = 0.20 trend to spherical grain growth type, but with very smaller size. These results agree with XRD results which showed that with increasing the Bi-content the grain size of crystalline particles decreases. However, at = $x \geq 0.20$ again crystallite size is increased.

3.3. Electrical properties

The results of electrical measurements for SnO_2: Bi thin films have been summarized in Table 2. Also, variation of resistivity (ρ) and carrier concentration (n) as a function of x are shown in Fig. 6. The resistivity of undoped SnO_2 film is 5×10^{-3} (Ω.cm). Apart from pure SnO_2 film, at first, resistivity of films was decreased with Bi-doping up to $x \leq 0.10$ and reached to about 2.3 Ω.cm at x = 0.10 and then it is increased in range $0.10 \leq x \leq 0.20$ to about 22.7 Ω.cm at x = 0.20. The initial reduction of resistivity is due to existent of Bi ions in Sn lattice sites and donor creation of Bi in SnO_2 lattice and later increase in resistivity might be due to the interstitial sites, mixed phases of Bi-Sn-O and unstable phases of Tin oxides such as Sn_3O_4 and Sn_5O_6 and therefore more disorder. But, again in $x \geq 0.20$, resistivity decreased

and reached to about 3.6 Ω.cm which related to energy band structure due to formation of Sn-O-Bi mixed phases or decrease of the E_g.

However, the intrinsic oscillation of resistivity related to phase structure change of films due to Bi-doping. This tendency in change of carrier concentration is seen, too.

Majority carrier concentration was calculated using the following equation by the Hall effect measurements [17]:

$n = IB/qV_H \times t$ (3)

where I, B, t, q and V_H are the measured current, magnetic flux density, film thickness, electron charge and Hall voltage, respectively. From the Hall effect experiment at room temperature (T = 300 K), it was found that the majority carriers were electrons for all doping levels (n-type conductivity).

3.4. Optical properties

The optical transmittance of the SnO_2: Bi films in wavelength range of λ = 300 to 1100 nm is shown in Fig. 7. Totally, the average transparency of films relatively decreased from ~ 84% to ~ 72% when x increases from 0 to 0.30. This behavior probably is due to presence of Bi-ions n SnO_2 lattice and scattering in grain boundaries and decreasing the crystalline size as it is expected from XRD analysis and SEM images. The doped sample deposited with x = 0.10 exhibits the highest transparency of about 80% in the visible region.

The optical energy gap (E_g) of the prepared films determined from the optical measurements. The absorption coefficient for the films found to follow the relation.

$\alpha = A (hv-Eg)^{m} / h v$ (4)

where A is constant, hv is the incident photon energy, m depends on the nature of band transition; m = 1/2 or 3/2 for direct allowed and direct forbidden transitions, and m = 2 or 3 for indirect allowed and indirect forbidden transitions [17, 21]. From the $(\alpha hv)^2$ versus hv plots, the intercept obtained by the extrapolation of the linear region to α = 0 gives the direct band gap (E_g) of the films (Fig. 8). The values of E_g were obtained in range of 3.52–3.88 eV (Table 2). E_g gradually decreased with increasing Bi-doping level from x = 0 to x = 0.30.

This change of Eg may be attributed to many body effects so that with decreasing carrier concentration, the energy gap is also decreased [21].

3.5. Photoconductive properties

To investigate the photoconductivity of a semiconductor thin films, the sample is exposed to light at a certain wavelength. Then, a pair of electron and hole are produced with absorbing light energy in

semiconductor and exciting the electrons to the conduction band. Therefore, the density of free electron carriers (holes) increases and as a result, the electrical conductivity increases. This phenomenon is known as photoconductivity in semiconductor physics. In this experiment, resistance of the prepared films was obtained (under lighting) at specified time intervals at room temperature. The variation of relative resistance of the films (ΔR/R) with illumination versus exposure time and Bi-doping are shown in Fig. 9. As seen, photoconductivity of the films is increased with increasing exposure time. Resistance of SnO_2: Bi films decreases immediately after exposure to light. Photoconductivity increases when the Bi-doping level increases from x = 0 to x = 0.20 and then it decreases. Thus, the exposure time and doping level have significant influence on the photoconductivity of the films. The film deposited with x = 0.20 exhibited more photoconductivity than the other prepared films.

3.6. Thermoelectric properties

Thermoelectric materials transform thermal energy into electrical energy. Although n or p-type metal oxides with acceptable electrical conductivity [40] are found for use in thermoelectric applications, studies are still needed to develop these materials.

The figure of merit of a material's is expressed according to Eq. 5:

$ZT = S^2\sigma T / k$, **(5)**

Where S is the Seebeck coefficient, σ is the electrical conductivity, κ is the thermal conductivity, and T is the temperature. The value of $S^2\sigma$ is the power factor that can be used to approximate the thermal performance. According to Eq. 5, to produce high quality thermoelectric composites, materials must have high electrical conductivity and low thermal conductivity. Therefore, to increase the thermoelectric efficiency of a composite material, it is necessary to consider high S and σ values and low κ values. However, one of the problems related to the efficiency of thermoelectric materials is the coordination of electrical and thermal conductivity due to the ZT relationship, which affects the capabilities of thermoelectric materials [41]. In general, the scattering of phonons in the lattice reduces the thermal conductivity, and the addition of n or p type semiconductors to the oxide material can be effective in increasing/decreasing the electrical conductivity of the composite material. In other words, due to the complex relationship between conductivity and thermal parameters, it is difficult to increase the value of ZT by adjusting these parameters.

To improve the thermoelectric properties, factors such as effective mass, charge carrier density and carrier mobility play an important role. Because increasing temperature, the mobility of carriers also increases. Therefore, the carrier moves from a higher temperature site to a lower temperature and a greater thermoelectric potential occurs [42].

Wiedemann-Franz law was used to calculate the ZT coefficient. According to Wiedmann-Franz's law, in a semiconductor the relationship between thermal conductivity (k) and electrical conductivity (σ) is according to Eq. 6 [42, 43]:

$L = K / \sigma T$ **(6)**

Where T is the absolute temperature and L, Lorenz number $\left(L = \frac{\pi^2 K_B^2}{3e^2} = 2.45 \times 10^{-8} W\Omega K^{-2}\right)$, k_B Boltzmann constant, and e electron charge are often used for thermoelectric materials [43].

Figure 10. presents the variation of the Seebeck coefficient versus temperature for SnO_2: Bi films. The slope of these diagrams determines the conduction type. If the temperature difference ΔT between the two ends of a material is small, then the Seebeck coefficient of a material is defined as:

$S = \Delta V/\Delta T$ **(7)**

where ΔV is the thermoelectric voltage seen at the terminals. As a result, in p-type semiconductors (which have only holes mobile charges), S is positive. Likewise, in n-type semiconductors (which have only negative mobile charges or electrons), S is negative.

As seen in Fig. 9. thermoelectric (emf) increases in negative direction (n-type conductivity) for all films apart from x = 0.30 in agreement with Hall's experiment at room temperature. In 0.30 Bi-doping level, initially, thermoelectric (emf) increases in negative direction and then increases in positive direction (p-type conductivity) at temperature difference equal to ΔT = 80 K. Indeed, we expect that with applying a thermal field to film, trapped holes in lattice become free and majority carriers change from electron to hole. This problem may be related to creating holes in temperature difference more than ΔT = 80K, through oxygen vacancy due to releasing the O^{-2} ions at high temperature (See Fig. 9) [22, 23]. The highest Seebeck coefficient was obtained equal to 325 μVK^{-1} for a prepared film with x = 0.20. Also, values of σ, K, Seebeck coefficient and of figure of merit are reported in Table 3. The results in Table 3 show that when Bi is doped in SnO_2 thin film, the electrical conductivity as well as the thermal conductivity calculated using Widmann-Franz's law have the lowest value for the sample x = 0.20 and the maximum value without the doped sample, and the value of figure of merit for x = 0.20 is 1.85, which is higher than the other samples. We know that the thermal conductivity of the samples depends mainly on the lattice contribution. Since the atomic weights and atomic radii of Sn and Bi are different (atomic weight Sn:Bi = 118.71:208.98 amu, and atomic radii Sn:Bi = 140:156 pm), the reduction in thermal conductivity in the sample x = 0.20 can be mainly attributed to the increase in phonon scattering in the crystal lattice.

Conclusions

In this paper, the preparation and characterization of Bi-doped SnO_2 thin films is reported. These films have been deposited on glass substrates by spray pyrolysis technique. The structural, morphological, electrical, optical, thermoelectric and photoconductive properties of prepared films have been investigated. The results are characterized as following:

(a) It is observed that the physical properties of films strongly depend on the [Bi/Sn] concentrations in the deposition solution. The prepared low Bi-doped films exhibited a preferential growth along the (211) direction with a tetragonal rutile SnO_2 phase. The films deposited with x = 0.05 exhibited better crystallinity than the other prepared films.

(b) The SEM images, indicated that nanostructure of the condensed films has a particle-cluster growth type with nearly uniform surface.

(c) The minimum sheet resistance (Rs) and maximum carrier concentration (n) were obtained equal to 39.3 (KΩ/□) and 4.53×10^{18} cm^{-3}, respectively, for the film deposited with x = 0.10. The majority carrier concentration (n) was obtained in order of 10^{16}–10^{18} cm^{-3}, using Hall effect measurements for Bi-doped SnO_2 films.

(d) The thermoelectrical measurements showed that thermoelectric (emf) continuously increased in negative direction (n-type conductivity) for all films except for x = 0.30 Bi-doped SnO_2 film. The film deposited with x = 0.20 exhibited the best thermoelectric properties than the other samples. The Seebeck coefficient and figure of merit was obtained equal 325 μVK^{-1} and1.85, respectively, for x = 0.20 Bi-doped SnO_2 film.

(e) The transparency of the films decreased about 10%, as x increased from 0 to 0.30. The prepared film with x = 0.02 exhibited the highest optical transparency in the visible region.

(f) The band gap values were obtained in the range of 3.52–3.88 eV for direct allowed transitions.

(g) Photoconductivity studies showed that the exposure time and Bi-doping play a very important role on the photoconductive property. Also, the best photoconductive property was obtained for the film deposited with x = 0.20.

These results showed that Bi doping modified the physical properties of the SnO_2 thin films and making it suitable for semiconductor devices applications such as photoconductivity, thermoelectric and sensor devices.

References

[1] H. He, Z. Yang, Y. Xu, et al., Perovskite oxides as transparent semiconductors: a review, Nano Convergence 7, 32 (2020). https://doi.org/10.1186/s40580-020-00242-7

[2] Sh. Li, M. Pomaska, A. Lambertz, W. Duan, et al.,Transparent-conductive-oxide-free front contacts for high-efficiency silicon heterojunction solar cells, Joule, 5 (2021) 6, 1535-1547, https://doi.org/10.1016/j.joule.2021.04.004

[3] T. Zinchenko, E. Pecherskaya, D. Artamonov, The properties study of transparent conductive oxides (TCO) of tin dioxide (ATO) doped by antimony obtained by spray pyrolysis, AIMS Materials Science, 2019,

6(2): 276-287. doi: 10.3934/matersci.2019.2.276

[4] R.A. Afre, N. Sharma, M. Sharon and M. Sharon, Transparent conducting oxide films for various applications: a review, Rev.Adv. Mater. Sci. 53 (2018) 79-89.

[5] A.L. Dawar, A.K. Jain, C.J. Jagadish, H. Hartnagel, Semi-conducting Transparent Thin Films, IOP, Bristol, 1995

[6] T. Ma, M. Nikiel, A.G. Thomas, et al., A novel and potentially scalable CVD-based route towards SnO_2:Mo thin films as transparent conducting oxides. J Mater Sci 56, 15921–15936 (2021). https://doi.org/10.1007/s10853-021-06269-3.

[7] Y. Xueai, F. Weiwei, and Z. Xin, Preparation and photoelectric properties of Zn_2SnO_4-based composite nanomaterials, Emerging Materials Research 4 (2020) 3, 991-999, https://doi.org/10.1680/jemmr.20.00103

[8] N.E. Sung, H. J. Shin, K. H. Chae, S. O. Won, I.J. Lee, Epitaxial Zinc Stannate (Zn_2SnO_4) Thin Film for Solar Cells, ACS Appl. Energy Mater. 2020, 3, 7, 6056−6059, https://doi.org/10.1021/acsaem.0c00461

[9] Sh.P. Chang, W.D. Chen, W.L. Huang, nvestigation of $MgIn_2O_4$ MSM UV Photodetector Wif Different Oxygen Flow Ratios and Post-Annealing Temperatures, *ECS J. Solid State Sci. Technol.* 10 (2021) 055014, https://doi.org/10.1149/2162-8777/ac0115

[10] Yanagawa K, Ohki Y, Omata T, Hosono H, Ueda N and Kawazoe, Preparation of Cd1−xYxSb2O6 thin film on glass substrate by radio frequency sputtering, H. Appl. Phys. Lett. 65 (1994) 406, https://doi.org/10.1063/1.112316.

[11] K. Fujiwara, H. Minato, J. Shiogai, A. Kumamoto, N. Shibata, A. Tsukazaki, Thin-film stabilization of $LiNbO_3$-type $ZnSnO_3$ and $MgSnO_3$ by molecular-beam epitaxy, APL Materials 7, 022505 (2019); https://doi.org/10.1063/1.5054289

[12] K. S. Gour, V. Karade, J. S. Jang, E. Jo, P. Babar, S. Korade, H. Yoo, S. Kim, D. Kim, J. Park, J. H. Kim, Nanoscale Rear-Interface Passivation in $Cu_2ZnSn(S,Se)_4$ Solar Cells through teh $CuAlO_2$ Intermediate Layer, ACS Applied Energy Materials 4 (2021)5, 5222-5229, DOI:10.1021/acsaem.1c00743

[13] M. Duinong, F. P. Chee, S. Salleh, A. Alias, K. A. Mohd Salleh, S. Ibrahim, Structural and Optical Properties of Gamma Irradiated $CuGaO_2$ Thin Film deposited by Radio Frequency (RF) Sputtering, *J. Phys.: Conf. Ser.* 1358 (2019) 012047.

[14] Ch.L. Yu, Ch.H. Weng, R.J. Huang, S. Sakthinathan, T.W. Chiu and Ch. Dong, Preparation of $CuCrO_2$ Anisotropic Dela-fossite-Type Thin Film by Electrospinning on Glass Substrates, Ceramics 2021, 4, 364–377. https://doi.org/10.3390/ceramics4030026

[15] S. Shet, K.S. Ahn, R. Nuggehalli, Y.Yana, J.Turner, M. Al-Jassim, Phase separation in Ga and N co-incorporated ZnO films and its effects on photo-response in photoelectrochemical water splitting, Thin Solid Films, 519, (2011) 18, 5983-5987, https://doi.org/10.1016/j.tsf.2011.03.050.

[16] A. Kumar, P.P. Sahay, Lithium doping in spray-pyrolyzed NiO thin films: results on their microstructural, optical and electrochromic properties. Appl. Phys. A 127, 286 (2021). https://doi.org/10.1007/s00339-021-04436-6.

[17] H. Azimi Juybari M.-M. Bagheri-Mohagheghi, S.A. Ketabi, M. Shokooh-Saremi, Fabrication and characterization of transparent p–n and p–me–n heterojunctions prepared by spray pyrolysis technique: TEMP Effect of post-annealing process and intrinsic middle layer, Physica E 43 (2010) 93–96.

[18] T.W. Chiu, K. Tonooka, N. Kikuchi, Fabrication of transparent $CuCrO_2$: Mg/ ZnO p-n junctions prepared by pulsed laser deposition on glass substrate, Vacuum 83 (2008) 614-616.

[19] S.F. Ahmed, S. Khan, P.K. Ghosh, M.K. Mitra, K.K. Chattopadhyay, J. Sol–Gel Sci. Technol. 39 (2006) 241.

[20] M. M. Bagheri-Mohagheghi, M. Shokooh-Saremi, Electrical, Optical and Structural Properties of Li-Doped SnO_2 Transparent Conducting Films Deposited by teh Spray Pyrolysis Technique: A Carrier-Type Conversion Study, Semiconductor Science and Technology, Semicond. Sci. Technol. 19 (2004) 764, https://doi.org/10.1088/0268-1242/19/6/019.

[21] M.-M. Bagheri-Mohagheghi, M. Shokooh-Saremi, The electrical, optical, structural and thermoelectrical characterization of n-and p-type cobalt-doped SnO_2 transparent semiconducting films prepared by spray pyrolysis technique, Physica B 405 (2010) 4205–4210.

[22] Tagreed M.Al-Saadi, Bushra H.Hussein, Alaa B. Hasan, A.A.Shehab, Study the Structural and Optical Properties of Cr doped SnO_2 Nanoparticles Synthesized by Sol-Gel Method, Energy Procedia,157 (2019) 457-465, https://doi.org/10.1016/j.egypro.2018.11.210.

[23] P.P. Filippatos, N. Kelaidis, M. Vasilopoulou, D. Davazoglou , A. Chroneos, Impact of boron and indium doping on teh structural, electronic and optical properties of SnO_2 Scientific Reports,11 (2021)13031. https://doi.org/10.1038/s41598-021-92450-2.

[24] M. Hasan Zadeh Maha, M.-M. Bagheri-Mohagheghi , H. Azimi-Juybari, Tin doped β-In_2S_3 thin films prepared by spray pyrolysis: Correlation between structural, electrical, optical, thermoelectric and photoconductive properties, Thin Solid Films 536 (2013) 57–62, https://doi.org/10.1016/j.tsf.2013.03.047.

[25] T. Indira Gandhi, R. Ramesh Babu and K. Ramamurthi, Structural, morphological, electrical and optical studies of Cr doped SnO_2 thin films deposited by teh spray pyrolysis technique, Materials Science in Semiconductor Processing 16 (2013) 472-479.

[26] K Ravichandran, K Thirumurugan, Type Inversion and Certain Physical Properties of Spray Pyrolysed SnO_2:Al Films for Novel Transparent Electronics Applications, Journal of Materials Science & Technology, 2014, 30 (2), 97-102, https://doi.org/10.1016/j.jmst.2013.09.019.

[27] Chinnappa, L.; Ravichandran, K.; Saravanakumar, and et.al., The combined effects of molar concentration of the precursor solution and fluorine doping on the structural and electrical properties of tin oxide films, Journal of materials science: materials in electronics (2011) 22:1827-1834.

[28] E. Mokaripoor, M.-M. Bagheri-Mohagheghi, Study of structural, electrical and photoconductive properties of F and P co-doped SnO2 transparent semiconducting thin film deposited by spray pyrolysis, Materials Science in Semiconductor Processing 30 (2015) 400-405.

[29] G. Muruganantham, K. Ravichandran, K. Saravanakumar, A. T. Ravichandran, B. Sakthivel, TEMPEffect of solvent volume on the physical properties of undoped and fluorine doped tin oxide films deposited using a low-cost spray technique, Superlattices and Microstructures 50 (2011) 722-733.

[30] Ha-Rim An, ChangYeoulKim, Sung-TagOh, Hyo-JinAhn, Effect of sol-layers on Sb-doped SnO_2 thin films as solution-based transparent conductive oxides, Ceramics International 40 (2014) 385-391,DOI:10.1016/j.ceramint.2013.06.013

[31] Sushant Gupta, B.C. Yadav, Prabhat K. Dwivedi, B. Das, Microstructural, optical and electrical investigations of Sb-SnO_2 thin films deposited by spray pyrolysis, Materials Research Bulletin 48 (2013) 3315-3322. DOI:10.1016/j.materresbull.2013.05.001

[32] Wenhao Yang, Shihui Yu, Yang Zhang, Weifeng Zhang, Properties of Sb-doped SnO_2 transparent conductive thin films deposited by radio-frequency magnetron sputtering, Thin Solid Films 542 (2013) 285-288,DOI:10.1016/j.tsf.2013.06.077.

[33] T. Tsubota, S. Kobayashi, N. Murakami, T. OHNO, Improvement of Thermoelectric Performance for Sb-Doped SnO_2 Ceramics Material by Addition of Cu as Sintering Additive. Journal of Elec Materi 43, 3567–3573 (2014). https://doi.org/10.1007/s11664-014-3227-x.

[34] S. Yanagiya, N. V. Nong, M. Sonne, N. Pryds, Thermoelectric properties of SnO2-based ceramics doped with Nd, Hf or Bi, in: AIP Conf. Proc., 2012: pp. 327–330. doi:10.1063/1.4731563.

[35] S. Yanagiya, N. V. Nong, J. Xu, M. Sonne, N. Pryds, Thermoelectric Properties of SnO_2 Ceramics Doped with Sb and Zn, J. Electron. Mater. 40 (2011) 674–677. doi:10.1007/s11664- 010-1506-8.

[36] T. Tsubota, S. Kobayashi, N. Murakami, T. Ohno, Improvement of Thermoelectric Performance for Sb-Doped SnO_2 Ceramics Material by Addition of Cu as Sintering Additive, J. Electron. Mater. 43 (2014) 3567–3573. doi:10.1007/s11664-014-3227-x.

[37] K. Rubenis, S. Populoh, P. Thiel, S. Yoon, U. Müller, J. Locs, Thermoelectric properties of dense Sb-doped SnO_2 ceramics, Journal of Alloys and Compounds, 692 (2016), 515-521, doi: 10.1016/j.jallcom.2016.09.062.

[38] Wang, Jing, Qin Chen, Xia Chun Zhu, Seok Je Lee, Kyoung Woo Park, and Chulg Yu Jhun, "Preparation and Thermoelectric Properties of Bi Doped $Ca_3Co_4O_9$ Based Thermoelectric Materials, Key Engineering Materials 783 (2018) 144–147, https://doi.org/10.4028/www.scientific.net/kem.783.144.

[39] An Introduction to the Study of Chemistry. Forgotten Books. p. 363.ISBN 978-1-4400-5235-4. Retrieved 21 June 2012.

[40] N. Wang, H. He, Y. Ba, C. Wan, K. Koumoto, Thermoelectric properties of Nb-doped $SrTiO_3$ ceramics enhanced by potassium titanate nanowires addition, J. Ceram. Soc. Jpn. 118, (2010)1098 – 1101.

[41] Yan Chen, Xiangnan Hou, Chunyan Ma, Yinke Dou, and Wentao Wu, Review of Development Status of Bi2Te3-Based Semiconductor Thermoelectric Power Generation, Advances in Materials Science and Engineering, Article ID 1210562, 9 pages, Volume (2018), https://doi.org/10.1155/2018/1210562

[42] Fan Xa, Rong Z, Yang F, Cai X, Han X, Li G: "Effect of process parameters of microwave activated hot pressing on the microstructure and thermoelectric properties of Bi2Te3-based alloys" Journal of Alloys and Compounds, 630 (2015) 282-287.

[43] By Yucheng Lan, Austin Jerome Minnich, Gang Chen, Zhifeng Ren, "Enhancement of Thermoelectric Figure-of-Merit by a Bulk Nanostructuring Approach" Adv. Funct. Mater, 20 (2010) 357–376.

Tables

Table 1
XRD parameters for Bi-doped SnO_2 films at (211) orientation.

Sample	2θ (˚)	Lattice distance (Å)	FWHM (˚)	Mean grain size (nm)
Un-doped SnO_2	51.761	1.7647	0.547	17.95
SnO_2:Bi (x = 0.05)	51.764	1.7646	0.411	23.90
SnO_2:Bi(x ≥ 0.10)				

Table 2

Electrical and thermoelectric measurements results of Bi-doped SnO_2 thin films.

x	Sheet resistance (R_s, kΩ/□)	Resistivity (ρ, Ω.cm)	Carrier concentration (n, cm^{-3})	Carrier Type (Hall effect)	Energy gap (E_g, eV)	Thickness (t, nm) Δt = ± 50
0.00	0.225	1.25×10^{-2}	4.86×10^{19}	(-)	3.88	~ 500
0.05	120.0	7.80	2.67×10^{17}	(-)	3.58	~ 650
0.10	39.3	2.35	4.53×10^{18}	(-)	3.56	~ 600
0.15	81.2	5.68	4.83×10^{16}	(-)	3.55	~ 700
0.20	264.0	22.44	1.50×10^{16}	(-)	3.52	~ 850
0.30	51.8	3.62	1.35×10^{18}	(-)	3.52	~ 700

Table 3. Results of measurement of thermoelectric properties of Bi-doped SnO_2 films

X	σ(Ω.cm)$^{-1}$ =1/ρ (×10^{-2})	K=LσT ($Wm^{-1}K^{-1}$) (×10^{-6})	S(μV/K)	S^2 σ ($Wm^{-1}K$) (×10^{-10})	ZT (T=300 K)
0.00	80	13.72	-198	313.63	0.68
0.05	12.82	2.2	-98.18	12.41	0.17
0.10	42.55	7.3	-86.1	31.54	0.13
0.15	17.6	3	-124	27.1	0.27
0.20	4.45	0.76	-325	47	1.85
0.30	27.62	4.74	+5.71	0.09	0.003

Figures

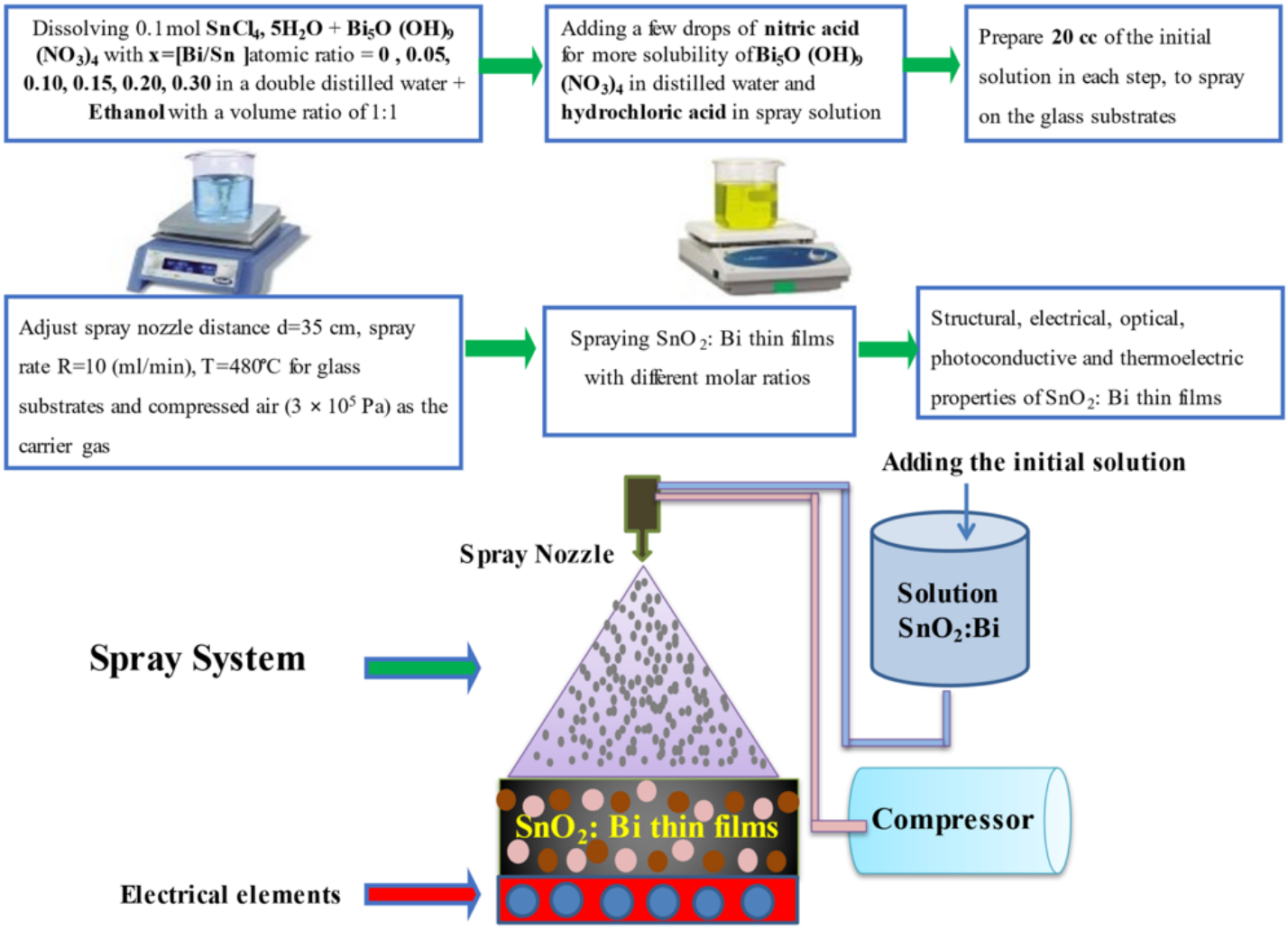

Figure 1

Flowchart of synthesis thin films of SnO2: Bi thin films with different ratio.

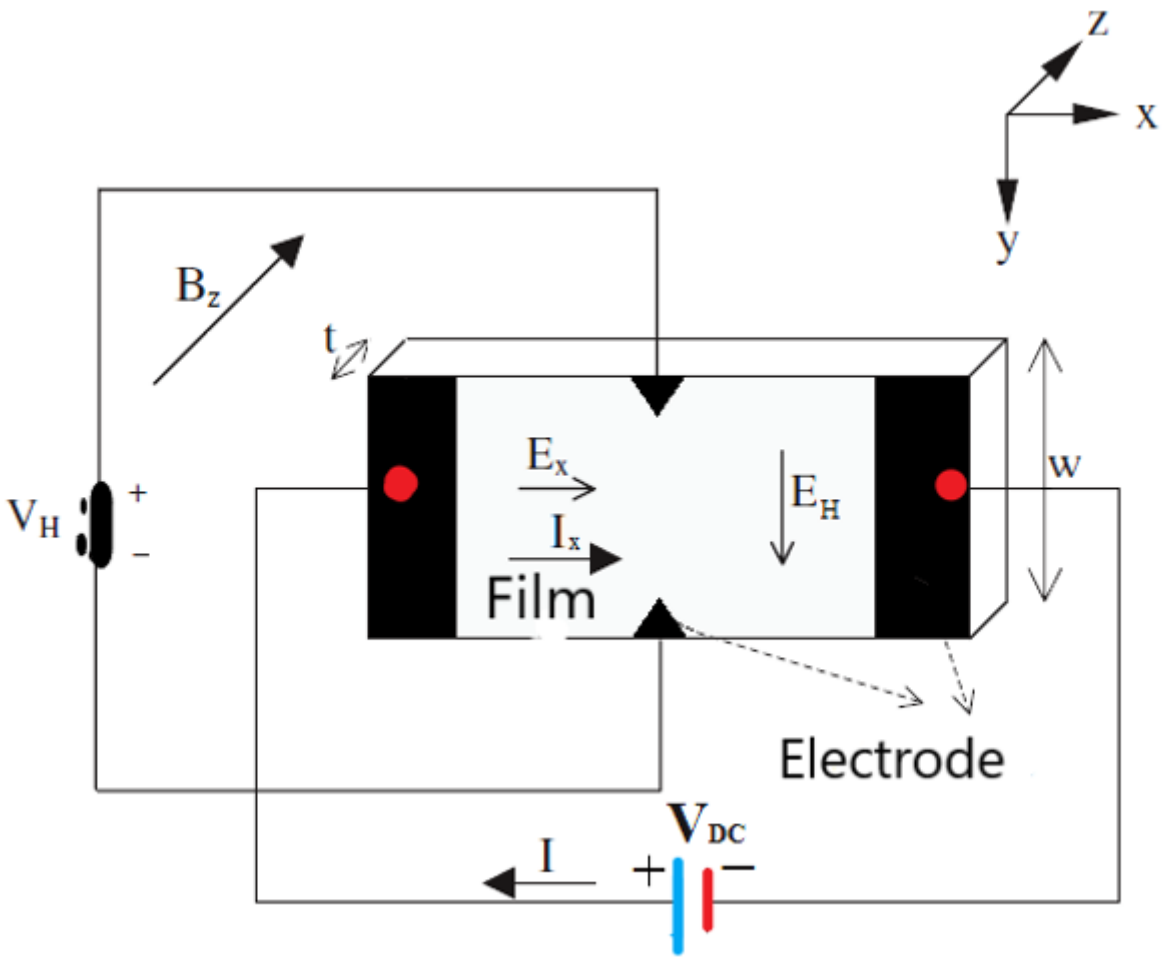

Figure 2

Basic setup for Hall effect experiment.

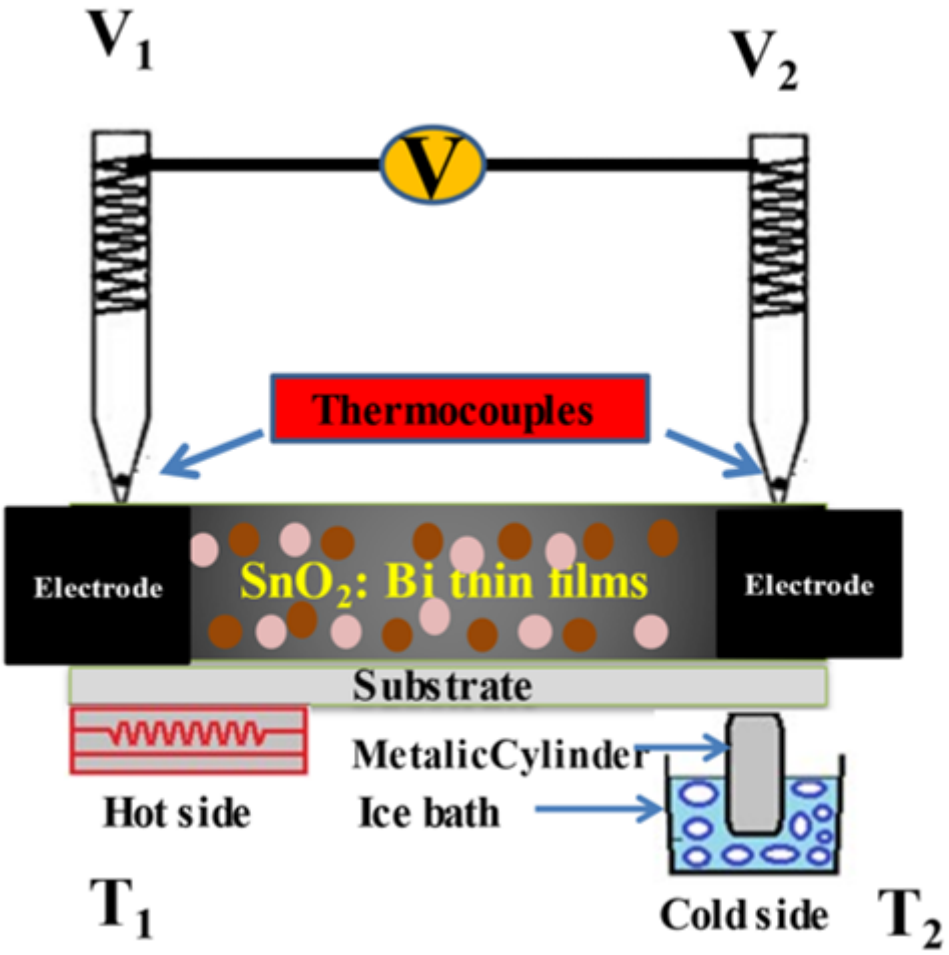

Figure 3

Simple configuration for thermoelectric power measurement.

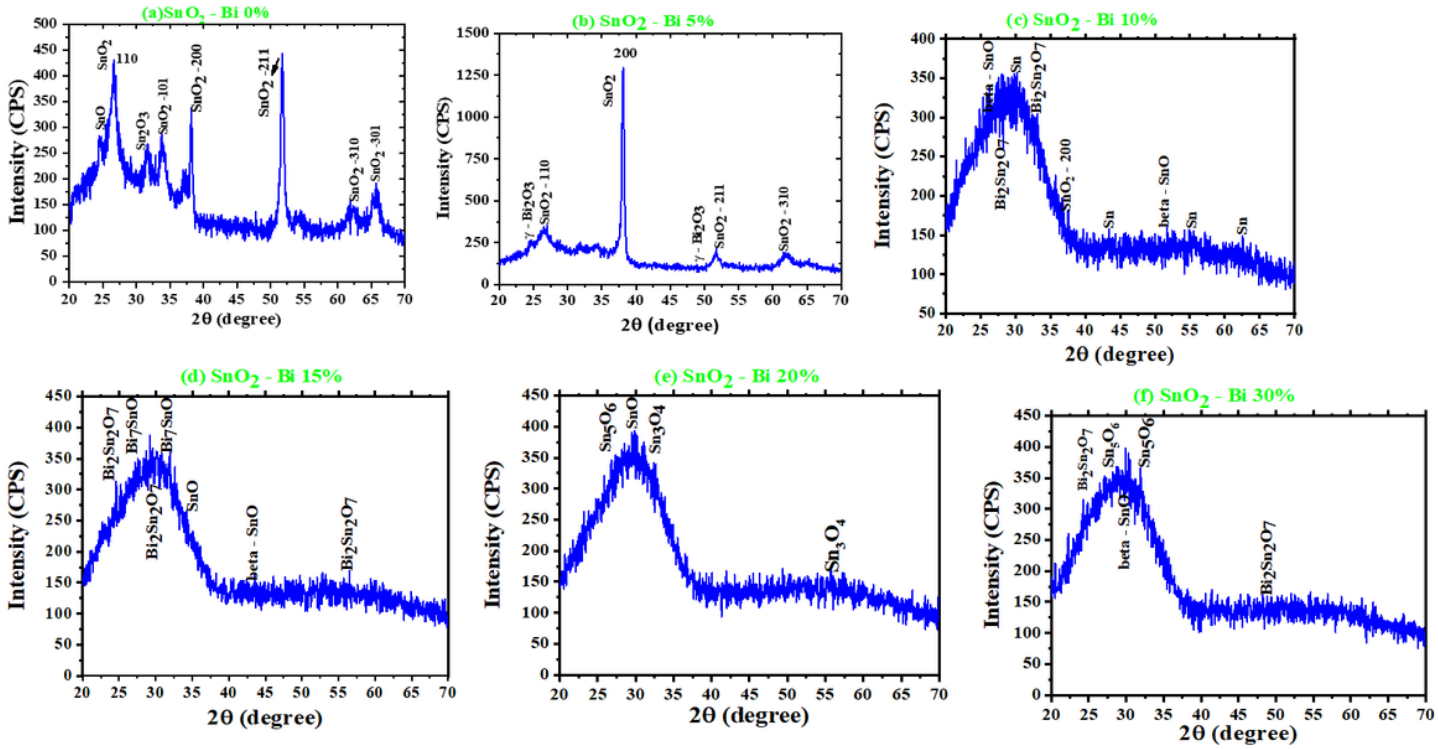

Figure 4

(a) - (f): XRD patterns of Bi-doped SnO2 with various concentrations of x=[Bi/Sn] at.%..

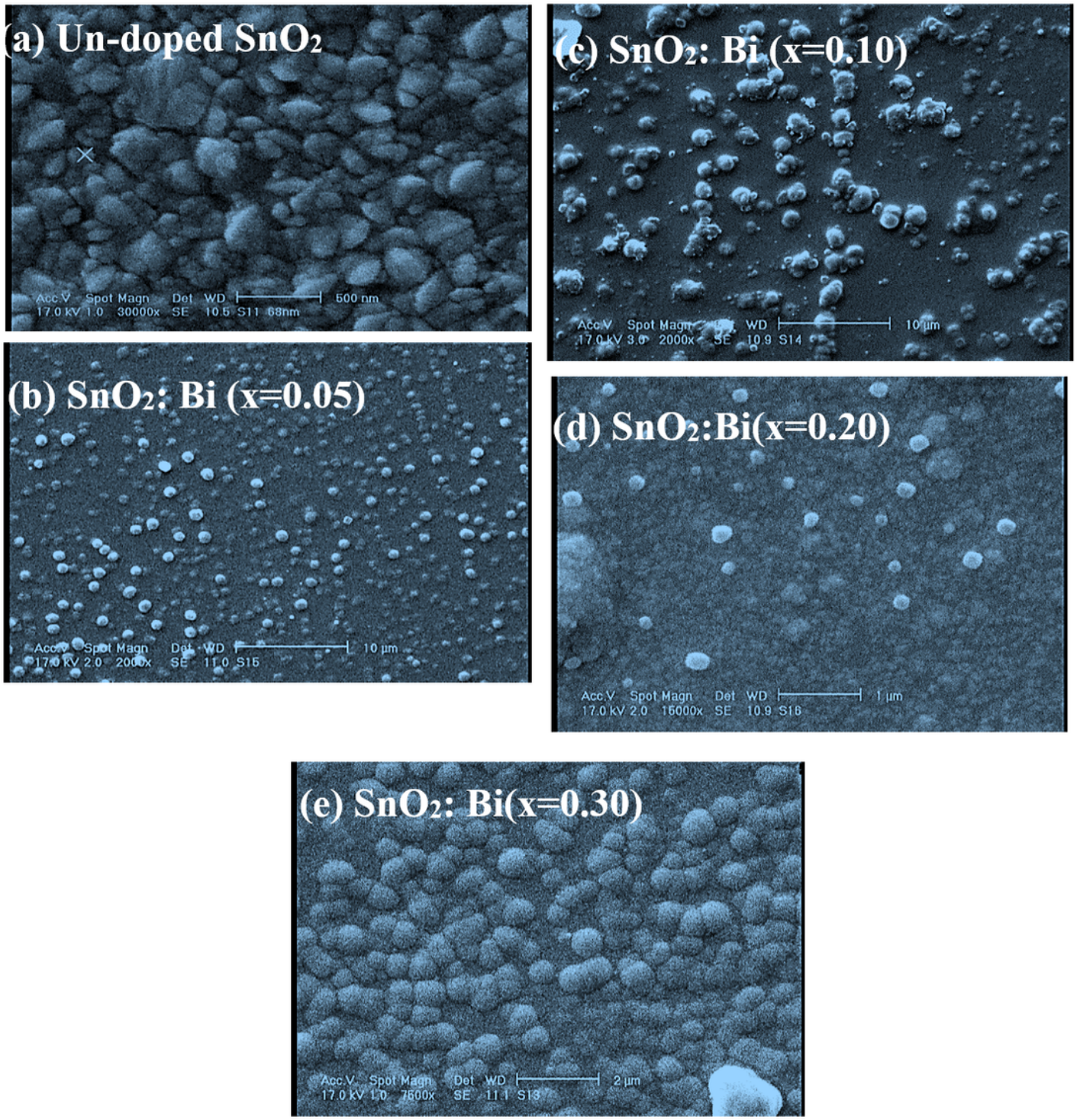

Figure 5

The SEM images of morphology of Bi-doped SnO2 films with various Bi- concentrations of x=[Bi/Sn] at.

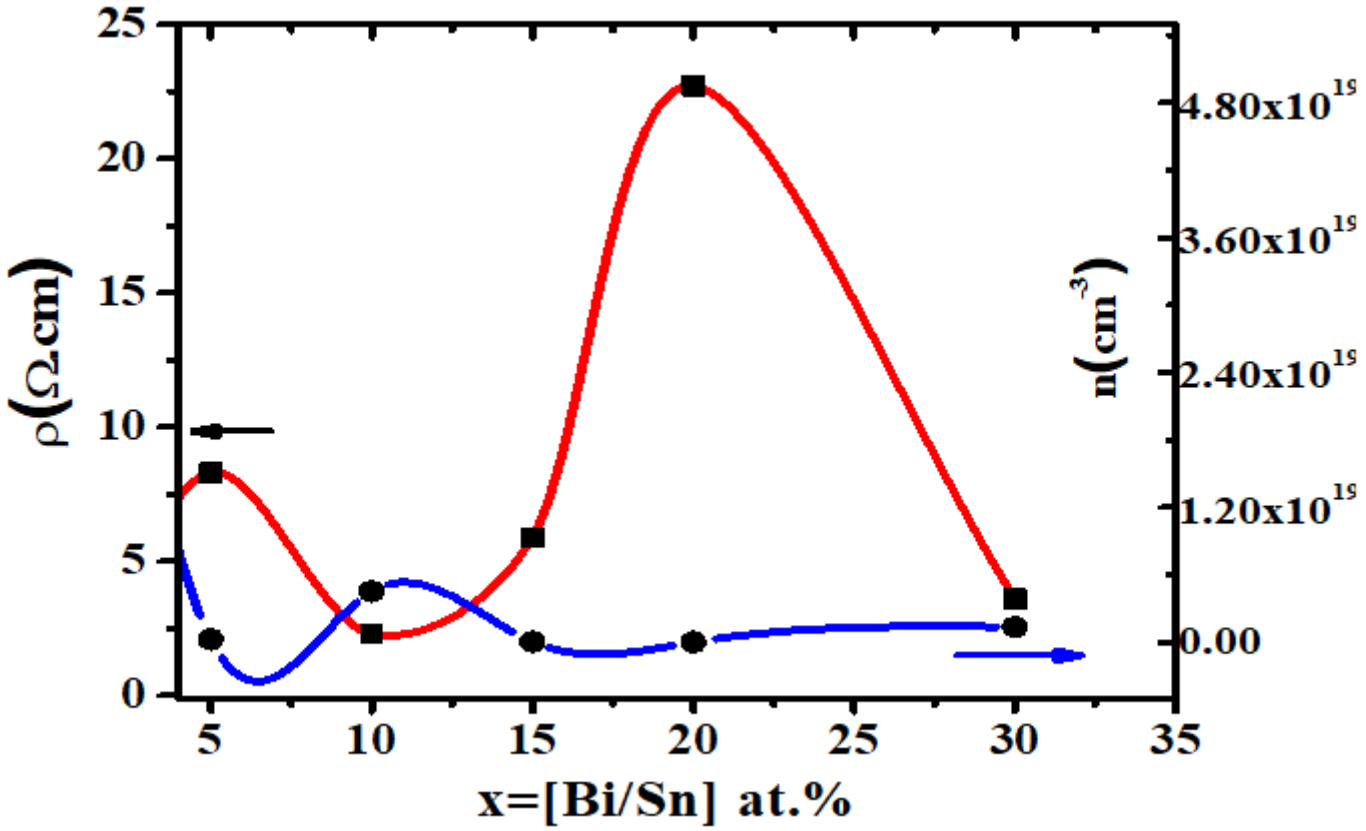

Figure 6

Variation of electrical resistivity and carriers concentration of SnO2:Bi thin films as function of x=[Bi/Sn] at.%..

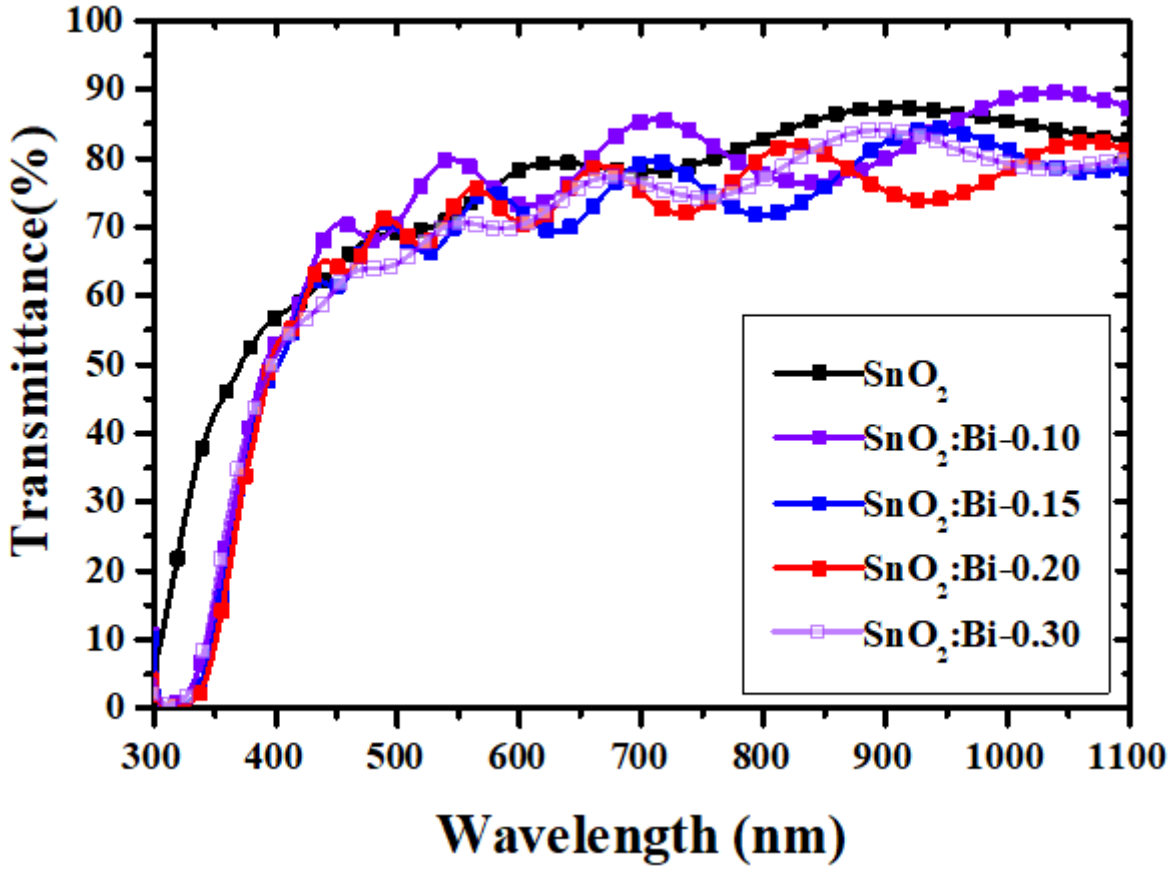

Figure 7

Optical transmittance of Bi-doped SnO2 films with different values of x=[Bi/Sn] at.

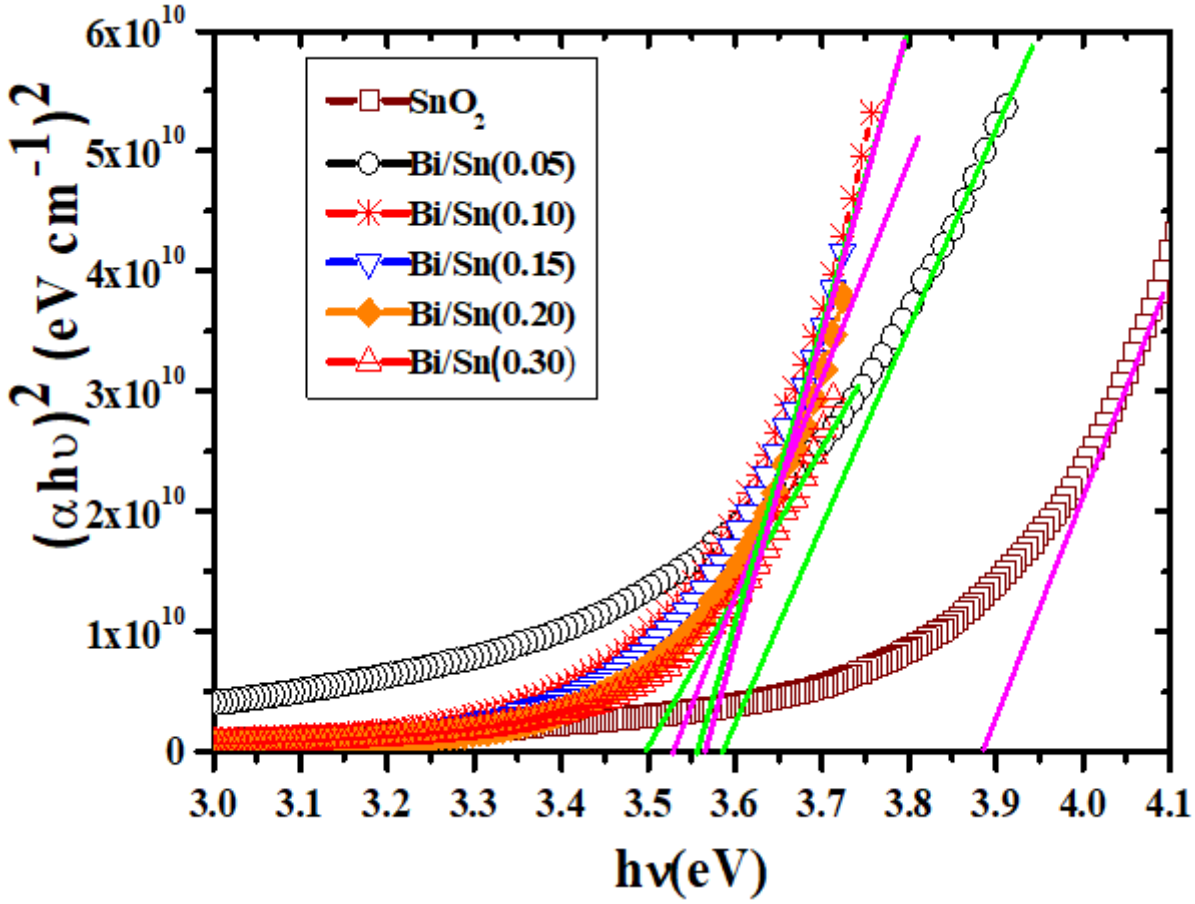

Figure 8

Plots of (αhυ)2 versus hυ for SnO2: Bi films with different values of x=[Bi/Sn] at.

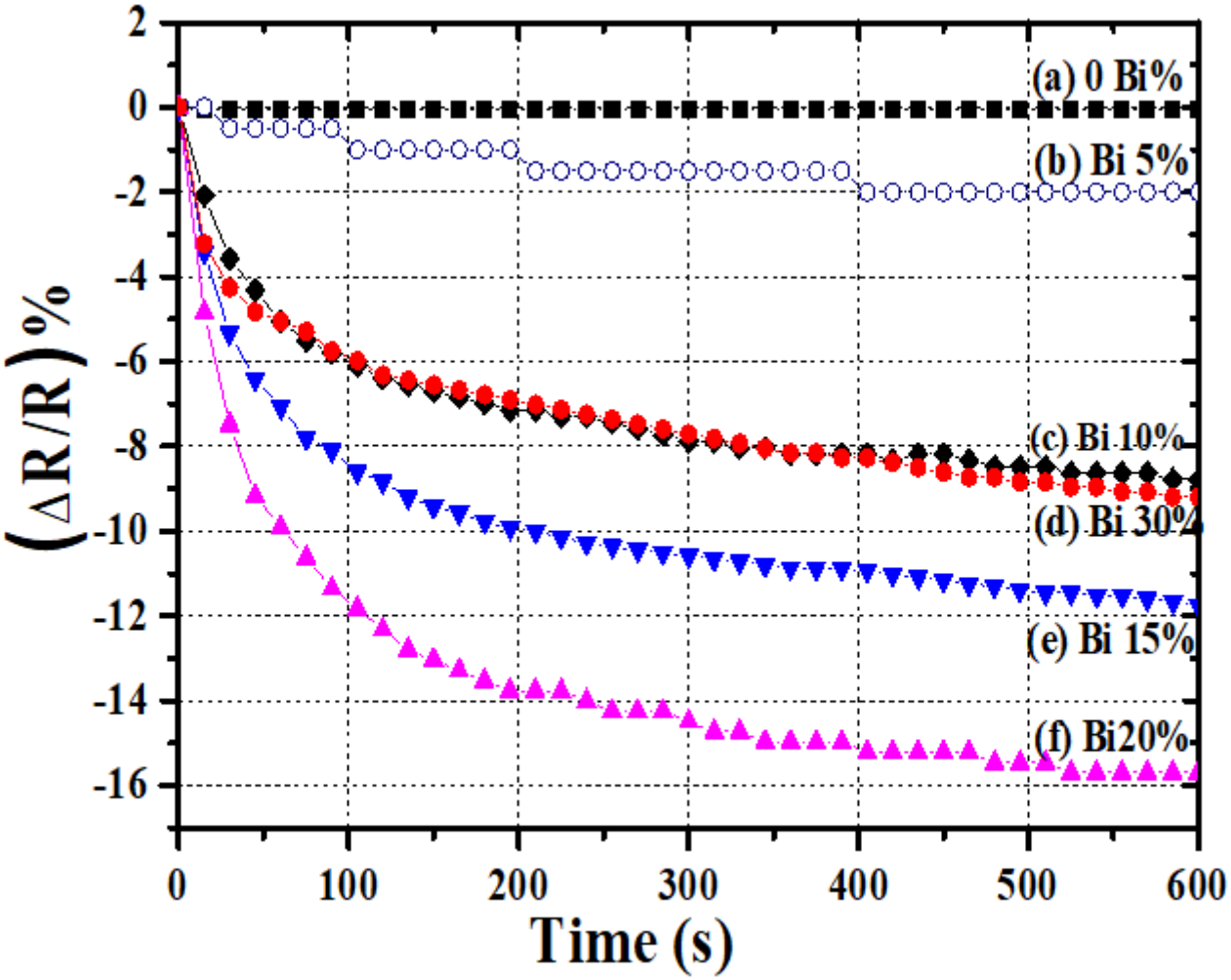

Figure 9

The relative change of sheet resistance versus light expo sure tXime for SnO2: Bi films with different values of x=[Bi/Sn] at.%.

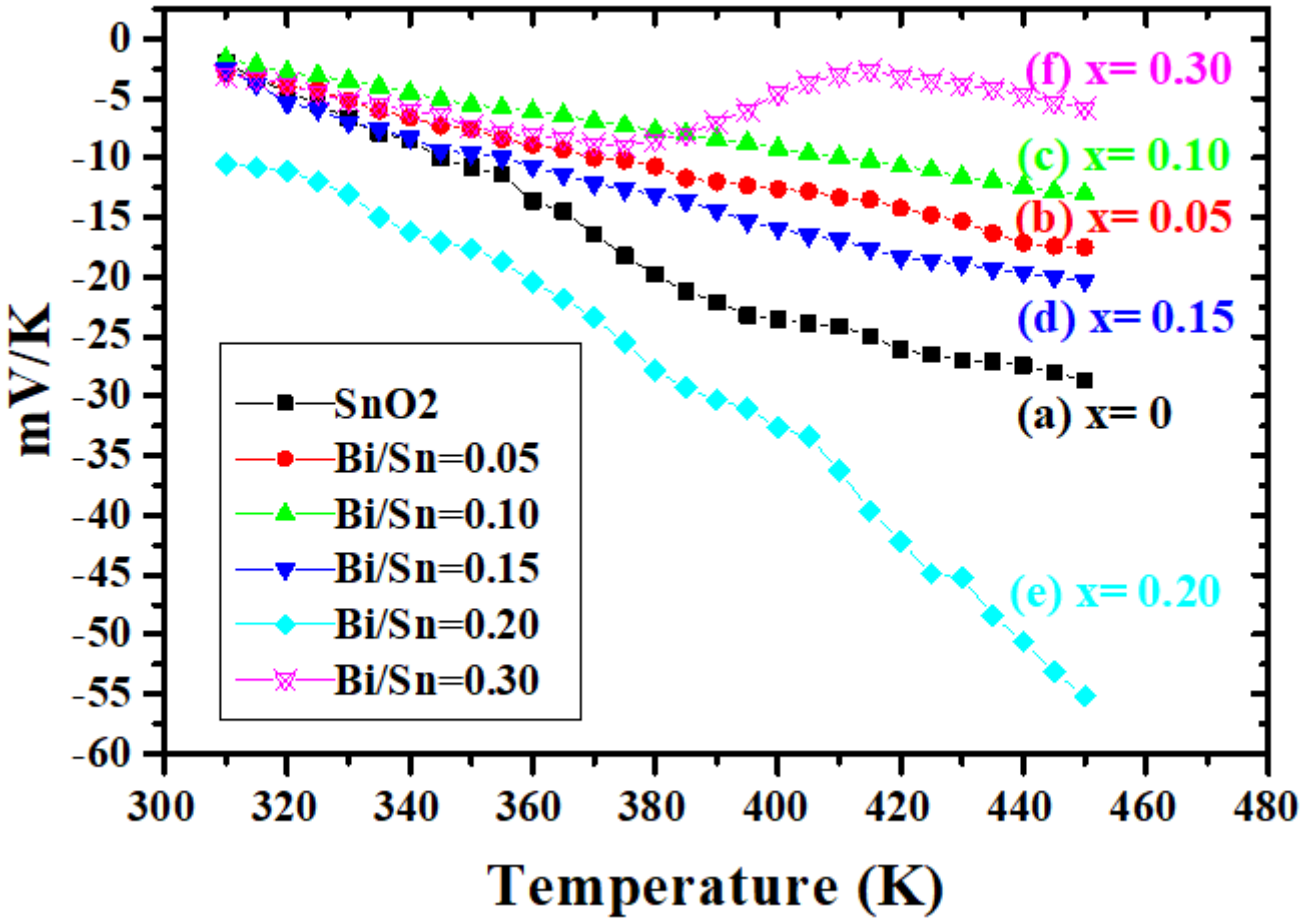

Figure 10

Behavior of thermoelectric voltage against temperature difference for SnO2:Bi films with different values of x=[Bi/Sn] at.